Acta Astronautica 66 (2010) 1506–1519

Contents lists available at ScienceDirect

Acta Astronautica

journal homepage: www.elsevier.com/locate/actaastro

Electric sail missions to potentially hazardous asteroids

Alessandro A. Quarta, Giovanni Mengali *

Dipartimento di Ingegneria Aerospaziale, University of Pisa, I-56122 Pisa, Italy

ARTICLE INFO

Article history:
Received 18 May 2009
Received in revised form
23 November 2009
Accepted 29 November 2009
Available online 24 December 2009

Keywords:
Electric sail
Trajectory optimization
Potentially hazardous asteroids exploration

ABSTRACT

Missions towards potentially hazardous asteroids require considerable propellant-mass consumption and complex flybys maneuvers with conventional propulsion systems. A very promising option is offered by an electric sail, an innovative propulsion concept, that uses the solar-wind dynamic pressure for generating a continuous and nearly radial thrust without the need for reaction mass. The aim of this paper is to investigate the performance of such a propulsion system for performing rendezvous missions towards all the currently known potentially hazardous asteroids, a total of 1025 missions. The problem is studied in an optimal framework by minimizing the total flight time. Assuming a canonical value of sail characteristic acceleration, we show that about 67% of the potentially hazardous asteroids may be reached within one year of mission time, with 137 rendezvous in the first six months. A detailed study towards asteroid 99942 Apophis is reported, and a comparison with the corresponding performance achievable with a flat solar sail is discussed.

1. Introduction

The Solar System contains a long-lived population of asteroids and comets, some fraction of which are perturbed into orbits that may cross the Earth's orbit. The potential threat posed by these objects of colliding with Earth may be so catastrophic that it is important to quantify the risk and prepare to deal with such a threat [1]. The first step in a program for the prevention or mitigation of impact catastrophes involves a search for potentially hazardous asteroids (PHAs) and a detailed analysis of their orbits. PHAs are classified on the base of parameters that measure the asteroid's potential to make threatening close approaches to the Earth [2]. In particular, all asteroids within an Earth minimum orbit intersection distance of 0.05 AU and an absolute visual magnitude of 22.0 or less are considered PHAs. Because the absolute magnitude depends on the asteroid's albedo, and since the albedo for most asteroids is not known, an albedo range between 0.25 and 0.05 is usually assumed [3], and this results in a range for the equivalent diameter of the asteroid whose minimum value is approximately 150 m. Although the annual likelihood that a PHA collides with Earth is extremely small [4], it is important to investigate mission scenarios whose purpose is to send a spacecraft near the asteroid [5,6] to leave it a transponder (or a reflector). In fact, tagging the asteroid may be necessary to track it accurately enough to determine the probability of a collision with Earth, and thus help decide whether to mount a deflection mission to alter its orbit [7,8]. In particular, in this paper we study the potentialities offered by an electric sail spacecraft to fulfill the rendezvous mission.

The electric sail is an innovative propulsion concept that uses the solar wind dynamic pressure for generating a thrust without the need for reaction mass [9–11]. The spacecraft is spun around a symmetry axis and uses the centrifugal force to deploy and stretch out a number of thin, long conducting tethers [12]. The latter are held at a high positive (or negative [13]) potential through an

* Corresponding author. Tel.: +39 050 2217220; fax: +39 050 2217244.
E-mail addresses: a.quarta@ing.unipi.it (A.A. Quarta), g.mengali@ing.unipi.it (G. Mengali).

0094-5765/$ - see front matter © 2009 Elsevier Ltd. All rights reserved.
doi:10.1016/j.actaastro.2009.11.021

Nomenclature

Symbols

A	state matrix
A_{ij}	generic entry of A (with $i=1,\ldots,6$ and $j=1,2,3$)
a_c	characteristic acceleration
$\boldsymbol{a}_s$	sailcraft propulsive acceleration ($\hat{\boldsymbol{a}}_s \triangleq \boldsymbol{a}_s/\\|\boldsymbol{a}_s\\|$)
$\boldsymbol{b}$	vector
b_i	generic entry of $\boldsymbol{b}$
c_1, c_2, c_3	auxiliary variables, see Eqs. (13)–(15)
f, g, h, k	modified equinoctial elements
J	performance index
H	Hamiltonian
H'	reduced Hamiltonian, see Eq. (9)
$\hat{\boldsymbol{i}}$	unit vector
L	true longitude
p	semilatus rectum
$\boldsymbol{r}$	sailcraft position vector ($r \triangleq \\|\boldsymbol{r}\\|$)
t	time
$\boldsymbol{v}$	velocity vector
$\boldsymbol{x}$	state vector
z	auxiliary complex variable, see Eq. (16)
α	sail cone angle
$\tilde{\alpha}$	unconstrained optimum cone angle, see Eq. (18)
δ	sail clock angle
Δt	flight time
ΔV	total variation of velocity (two-impulse transfer)
η	propulsive acceleration parameter ($\eta = 7/6$)
$\boldsymbol{\lambda}$	adjoint vector
$\mu_\odot$	Sun's gravitational parameter
ν	true anomaly
τ	switching parameter
$\mathcal{T}_{\mathrm{RTN}}$	radial-tangential-normal orbital reference frame
$\mathcal{T}_\odot$	heliocentric-ecliptic inertial frame

Subscripts

0	initial
1	final
$\star$	target asteroid
$\oplus$	Earth
c	coasting
max	maximum
min	minimum
ss	solar sail
t	transfer orbit

Superscripts

$\cdot$	time derivative
T	transpose

electron gun, whose electron beam is shot roughly along the spin axis. The resulting static electric field of the tethers perturbs the trajectories of the incident solar wind protons, thus producing a momentum transfer from the solar wind plasma stream to the tethers. The propelling thrust is almost radially directed, although a circumferential component can also be generated by inclining the sail plane at an angle with respect to the nearly radial solar wind flow. This is possible acting on tunable resistors, placed between the spacecraft and each tether, which allow each tether to slightly vary its potential. Because the thrust magnitude depends on the tether potential, the resistors provide a way to control the thrust experienced by each tether individually. As a result, the sail plane can be rotated by modulating the resistors settings with a sinusoidal signal synchronized to the spacecraft rotation. The electric sail thrust concept has been used to calculate successful and efficient mission trajectories in the Solar System for realistic payloads [12,14,15]. Missions towards PHAs represent an interesting option for an electric sail whose peculiar characteristics allows the spacecraft to fulfill transfers that otherwise will need either a considerable propellant mass [16] or significant complications such as planetary flybys [17–19]. Moreover, unlike conventional chemical propulsion systems [20], an electric sail offers some flexibility in the selection of the launch window, a feature that may be obtained also with a solar sail [21–25] and, to a lesser extent, with an electric propulsion system [26] and a mini-magnetospheric plasma thruster [27–29]. The aim of this paper is to provide a thorough analysis of electric sail potentialities to perform rendezvous missions towards any of the current catalogued PHAs. In particular, minimum time transfer trajectories are studied, aiming at emphasizing the relationships between the electric sail performance (in terms of characteristic acceleration) and the flight time. Moreover, a mission towards aspecific asteroid, 99942 Apophis, is analyzed in detail and a comparison is made with the results achievable using a flat solar sail.

2. Problem statement

Consider an electric sail whose state $\boldsymbol{x}$, at a generic time instant t, is defined through the modified equinoctial orbital elements (MEOE) p, f, g, h, k, and L as [30,31]

$$\boldsymbol{x} \triangleq [p, f, g, h, k, L]^{\mathrm{T}} \tag{1}$$

The sailcraft equations of motion can be written as [32,33]

$$\dot{\boldsymbol{x}} = A\boldsymbol{a}_s + \boldsymbol{b} \tag{2}$$

where $\boldsymbol{a}_s$ is the sailcraft propelling acceleration, $A \in \mathbb{R}^{6\times 3}$ and $\boldsymbol{b} \in \mathbb{R}^{6\times 1}$ are suitable matrices whose generic entries will be referred to as A_{ij} and b_i, respectively. An explicit expression for A_{ij} and b_i as a function of the MEOE is given in Appendix A.

The introduction of the modified equinoctial elements into the equations of motion allows one to significantly

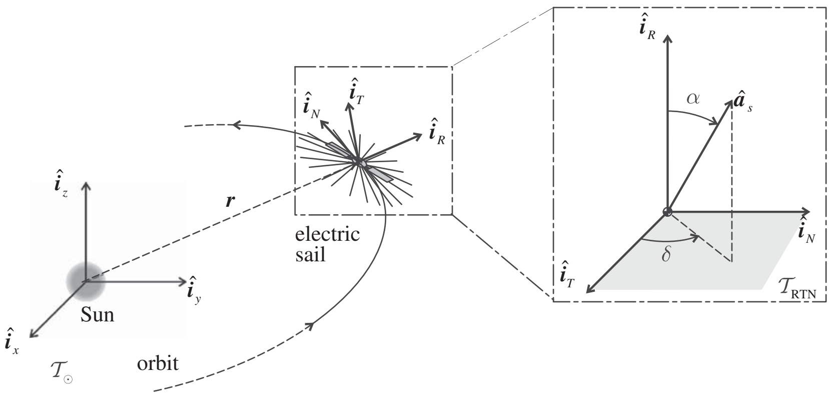

Fig. 1. Reference frames and electric sail control angles α and δ.

reduce the computational time necessary for the sailcraft trajectory integration. Also, it is useful to introduce a rotating radial-transverse-normal $\mathcal{T}_{\rm RTN}(\hat{\boldsymbol{i}}_R, \hat{\boldsymbol{i}}_T, \hat{\boldsymbol{i}}_N)$ orbital reference frame [32], whose unit vectors are

$$\hat{\boldsymbol{i}}_R = \frac{\boldsymbol{r}}{\|\boldsymbol{r}\|}, \quad \hat{\boldsymbol{i}}_N = \frac{\boldsymbol{r}\times\boldsymbol{v}}{\|\boldsymbol{r}\times\boldsymbol{v}\|}, \quad \hat{\boldsymbol{i}}_T = \hat{\boldsymbol{i}}_N \times \hat{\boldsymbol{i}}_R \tag{3}$$

where $\boldsymbol{r}$ and $\boldsymbol{v}$ are the sailcraft position and velocity vector. Let a_c be the electric sail characteristic acceleration, that is, the spacecraft maximum propelling acceleration at a distance of 1 AU from the Sun. The direction of the propelling acceleration is unambiguously defined through two independent control angles $\alpha \in [0, \alpha_{\max}]$ and $\delta \in [0, 2\pi]$. With the aid of Fig. 1 one has [12,14]

$$\boldsymbol{a}_s = a_c \tau \left(\frac{r_\oplus}{r}\right)^\eta \hat{\boldsymbol{a}}_s \quad \text{with } [\hat{\boldsymbol{a}}_s]_{\mathcal{T}_{\rm RTN}} = [\cos\alpha, \sin\alpha\cos\delta, \sin\alpha\sin\delta]^{\rm T} \tag{4}$$

where $\eta \triangleq 7/6$ [10], a_c is the characteristic acceleration (defined as the maximum propelling acceleration at 1 AU), and $r = \|\boldsymbol{r}\|$ is the Sun-sailcraft distance that, in terms of MEOE, is given by [33]

$$r = \frac{p}{1 + f\cos L + g\sin L} \tag{5}$$

while the switching parameter $\tau = (0,1)$, which models the electric sail on/off condition, is introduced to account for coasting arcs in the spacecraft trajectory. Note that the sailcraft thrust can be turned off ($\tau = 0$) at any time by simply switching off the electron gun.

From a geometrical point of view, the control angle δ, referred to as clock angle in analogy with the solar sail case, is the angle between $\hat{\boldsymbol{i}}_T$ and the projection of the propulsive acceleration unit vector $\hat{\boldsymbol{a}}_s$ in the $(\hat{\boldsymbol{i}}_T, \hat{\boldsymbol{i}}_N)$ plane, see Fig. 1. The sail cone angle α is the angle between the Sun-sailcraft line ($\hat{\boldsymbol{i}}_R$) and the sailcraft thrust direction $\hat{\boldsymbol{a}}_s$. The sail cone angle is upper constrained, for instability reasons, by a maximum allowable value, $\alpha_{\max} \triangleq \max(\alpha) < \pi/2$ [12]. The control angles α and δ define a conic region inside which the propelling thrust is constrained to lie. The axis of this region coincides with the Sun-sailcraft line, while the half-opening angle of the cone coincides with $\alpha_{\max}$. Finally note that the control angles α and δ affect the direction of $\boldsymbol{a}_s$, but do not influence its magnitude, which depends on the Sun-spacecraft distance only. The latter characteristic represents the main difference between an electric sail and a solar sail [34–36], whose propelling acceleration magnitude depends on the sail nominal plane orientation through $\cos\alpha$.

2.1. Trajectory optimization

Assume that at the initial time instant $t_0 \triangleq 0$ the sailcraft is placed on an orbit around the Sun coincident with the Earth's heliocentric orbit. This situation is representative of an electric sail deployment on a parabolic Earth-escape trajectory: that is, with zero hyperbolic excess energy ($C_3 = 0\,{\rm km}^2/{\rm s}^2$). Let $\nu_0 \in [0, 2\pi]$ be the sailcraft true anomaly at t_0. The initial state vector $\boldsymbol{x}_0 \triangleq \boldsymbol{x}(t_0)$ is given by

$$\boldsymbol{x}_0 = [p_\oplus, f_\oplus, g_\oplus, h_\oplus, k_\oplus, L_\oplus + \nu_0]^{\rm T} \tag{6}$$

where $p_\oplus$, $f_\oplus$, $g_\oplus$, $h_\oplus$, $k_\oplus$, and $L_\oplus$ are the Earth's MEOE at perihelion. The problem addressed here is to calculate the minimum flight time $\Delta t \triangleq t_1 - t_0 \equiv t_1$ necessary to transfer the sailcraft on a final orbit defined by the five MEOE $p_\star$, $f_\star$, $g_\star$, $h_\star$, and $k_\star$. This amounts to finding the optimal mission performance irrespective of the initial and final sailcraft positions at $t = t_0$ (parking orbit) and $t = t_1$ (target orbit), respectively. In other terms, as the ephemeris constraints are not taken into account, it is possible to calculate the orbit-to-orbit minimum flight time corresponding to a given sailcraft characteristic acceleration [24].

From a mathematical point of view, both the initial true anomaly ν_0 and the final true longitude $L_1 \triangleq L(t_1)$ are left free. The values of these two quantities are obtained as outputs of the optimization process. Once L_1 is found, the corresponding value of the true anomaly $\nu_1 \triangleq \nu(t_1) \in [0, 2\pi]$ on the target orbit is obtained as [33,37]

$$\nu_1 = L_1 - \arctan\left(\frac{k_\star}{h_\star}\right) - \arctan\left(\frac{g_\star h_\star - f_\star k_\star}{f_\star h_\star + g_\star k_\star}\right) \tag{7}$$

The minimum transfer time is calculated using an indirect approach, by maximizing the scalar functional J defined as

$$J \triangleq -t_1 \tag{8}$$

Recalling the vectorial equations of motion (2), the Hamiltonian H is given by

$$H = H' + \boldsymbol{b} \cdot \boldsymbol{\lambda} \tag{9}$$

where

$$H' \triangleq (A\boldsymbol{a}_s) \cdot \boldsymbol{\lambda} \tag{10}$$

is that portion of the Hamiltonian that explicitly depends on the control variables. In Eq. (9) $\boldsymbol{\lambda} \triangleq [\lambda_p, \lambda_f, \lambda_g, \lambda_h, \lambda_k, \lambda_L]^{\mathrm{T}}$ is the adjoint vector whose time derivative is provided by the Euler–Lagrange equation:

$$\dot{\boldsymbol{\lambda}} = -\frac{\partial H}{\partial \boldsymbol{x}} \equiv -\frac{\partial H'}{\partial \boldsymbol{x}} - \frac{\partial b_6}{\partial \boldsymbol{x}} \lambda_L \tag{11}$$

The explicit expression of the Euler–Lagrange equation is rather involved and is not reported here for the sake of conciseness.

From Pontryagin's maximum principle, the optimal control law $\tau(t)$, $\alpha(t)$, and $\delta(t)$, to be selected in the domain of feasible controls, is such that, at any time, the function H' is an absolute maximum. To this end, a more useful expression for H' is obtained from Eq. (10) by taking into account that some entries of A are equal to zero (Appendix A). The result is

$$H' = \tau[\sin\alpha(c_1 \sin\delta + c_2 \cos\delta) + c_3 \cos\alpha] \tag{12}$$

where

$$c_1 \triangleq \lambda_f A_{23} + \lambda_g A_{33} + \lambda_h A_{43} + \lambda_k A_{53} + \lambda_L A_{63} \tag{13}$$

$$c_2 \triangleq \lambda_p A_{12} + \lambda_f A_{22} + \lambda_g A_{32} \tag{14}$$

$$c_3 \triangleq \lambda_f A_{21} + \lambda_g A_{31} \tag{15}$$

Introduce the auxiliary complex quantity

$$z \triangleq c_2 + j c_1 \tag{16}$$

where j is the imaginary unit. Invoking the necessary conditions $\partial H'/\partial\delta = 0$, the clock angle δ is obtained as

$$\delta = \mathrm{Arg}(z) \tag{17}$$

where $\mathrm{Arg}(\cdot)$ is the value of the argument of z in the interval $(-\pi, \pi]$. Consider now the cone angle α. Invoking the necessary condition $\partial H'/\partial\alpha = 0$ and solving for α, yields

$$\tilde{\alpha} = \arctan\left(\frac{c_2 \cos\delta + c_1 \sin\delta}{c_3}\right) \tag{18}$$

where the clock angle δ is obtained through Eq. (17). The tilde over α represents the unconstrained value of the cone angle. Recalling that α cannot exceed $\alpha_{\max}$, the optimal control law is given by

$$\alpha = \begin{cases} \tilde{\alpha} & \text{if } \tilde{\alpha} \le \alpha_{\max} \\ \alpha_{\max} & \text{if } \tilde{\alpha} > \alpha_{\max} \end{cases} \tag{19}$$

We note in passing that the maximization of H' with respect to the two control angles α and δ amounts to the maximization of the projection of $\boldsymbol{a}_s$ along the direction of the vector $A^{\mathrm{T}}\boldsymbol{\lambda}$. This means that, as long as $\tilde{\alpha} \le \alpha_{\max}$, the optimal direction of the propelling acceleration is given by

$$\hat{\boldsymbol{a}}_s = \frac{A^{\mathrm{T}}\boldsymbol{\lambda}}{\|A^{\mathrm{T}}\boldsymbol{\lambda}\|} \tag{20}$$

The latter result coincides with the optimal control law for an electric propulsion system [38,39].

Finally, it may be checked that the optimal switching function τ that maximizes H' is obtained as

$$\tau = \begin{cases} 0 & \text{if } (A\hat{\boldsymbol{a}}_s) \cdot \boldsymbol{\lambda} < 0 \\ 1 & \text{if } (A\hat{\boldsymbol{a}}_s) \cdot \boldsymbol{\lambda} \ge 0 \end{cases} \tag{21}$$

where the thrust angles α and δ necessary to calculate the components of $\hat{\boldsymbol{a}}_s$ through Eq. (4) are given by Eqs. (17) and (19). The optimal control law for α, δ, and τ extends to a three-dimensional case a previous planar control law discussed in Refs. [12,15].

The electric sail motion is described by the six first order differential equations of motion (2) and the six Euler–Lagrange equations (11). The corresponding 12 boundary conditions at the initial (given) time and at the final (unknown) time, and the further transversality condition necessary to find the flight time t_1 are

$$p(t_0) = p_{\oplus}, \quad f(t_0) = f_{\oplus}, \quad g(t_0) = g_{\oplus}, \quad h(t_0) = h_{\oplus}, \quad k(t_0) = k_{\oplus}$$

$$p(t_1) = p_{\star}, \quad f(t_1) = f_{\star}, \quad g(t_1) = g_{\star}, \quad h(t_1) = h_{\star}, \quad k(t_1) = k_{\star}$$

$$\lambda_L(t_0) = \lambda_L(t_1) = 0, \quad H(t_1) = 1 \tag{22}$$

In particular, the conditions involving the adjoint variable λ_L state that both the initial (ν_0) and the final (ν_1) sailcraft angular positions are left free.

3. Missions towards PHAs

The optimal control problem described in the previous section has been solved to find the minimum time required by an electric sail with a characteristic acceleration of $1\,\mathrm{mm/s^2}$ to reach the orbit of each asteroid belonging to the set of currently known PHAs. Note that this scenario refers to a set of individual missions, and not to an asteroids tour (a mission to visit the whole population of PHAs). The solution of the boundary-value problem associated to the variational problem has been found through a hybrid numerical technique that combines genetic algorithms (to obtain an estimate of the adjoint variables), with gradient-based and direct methods to refine the solution [40]. In all of the simulations the target asteroid is assumed to describe a Keplerian motion around the Sun. Accordingly, the five MEOE that identify the target orbit (that is, $p_\star$, $f_\star$, $g_\star$, $h_\star$, and $k_\star$) are constant on the sailcraft transfer. The values of these orbital parameters have been retrieved by the Near Earth Object Program from Jet Propulsion Laboratory [41]. Because the PHAs list is continuously updated with the new available astronomical observations, the database used here corresponds to that available in Ref. [41] on February 2, 2009. This database contains 1025 asteroids whose classical orbital parameters (calculated with respect to the J2000 heliocentric-ecliptic reference frame) are summarized

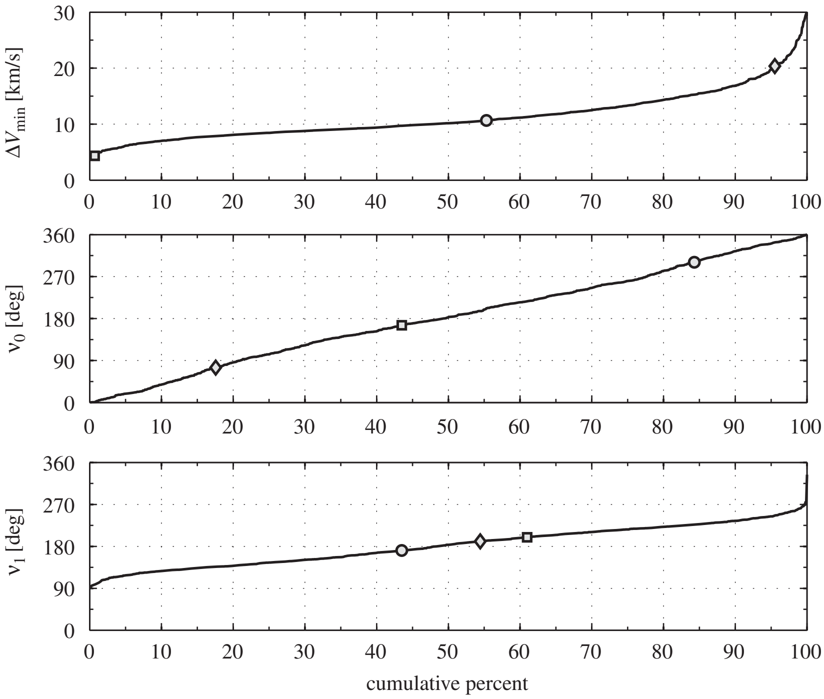

Fig. 2. Performance of an Earth-PHA optimum two-impulse transfer ($\square$ = 99942 Apophis, $\diamond$ = 3200 Phaethon, $\circ$ = 2101 Adonis).

in the table attached to this paper in electronic form (see Appendix B).

3.1. Optimal two-impulse transfers

To quantify the cost of a rendezvous mission towards the various PHAs, the total minimum ΔV variation (ΔV_{min}) for a two-impulse transfer has been preliminarily calculated. In fact, the value of ΔV_{min} for a two-impulse transfer of less than 360° is a measure of an asteroid accessibility [42]. The value of ΔV_{min} is obtained by solving a classical targeting problem between a point belonging to the Earth's heliocentric orbit (whose position is defined by the true anomaly $\nu_0 \in [0, 2\pi]$) and a second point belonging to the final orbit (characterized by the true anomaly $\nu_1 \in [0, 2\pi]$). Assuming a Keplerian motion, once the pair (ν_0, ν_1) is given, the total ΔV variation required by a two-impulse transfer is a function of p_t alone, the semilatus rectus of the transfer orbit. Therefore, ΔV_{min} can be found by minimizing the value of the total ΔV with respect to the three independent variables ν_0, ν_1, and p_t. The procedure implemented for the calculation of ΔV_{min} closely follows that described in [43] and used in [42] to analyze some trajectories towards near Earth asteroids. Note, however, that in [43] ΔV_{min} was found with respect to a standard Shuttle parking orbit around the Earth. Here, instead, the initial orbit coincides with the Earth's heliocentric orbit, and the escape phase from the Earth has not been included in the ΔV budget. The minimization of ΔV has been obtained using a direct method based on the use of the simplex algorithm [44].

The simulation results have been compared and validated with those calculated by the Advanced Concept Team (ACT) of European Space Agency.[1] The value of ΔV_{min}, along with the optimal initial and final angular positions of the sailcraft, is shown in the table attached to the paper and are graphically summarized in Fig. 2 in terms of cumulative percent. The figure shows three particular asteroids representative of small (99942 Apophis), medium (3200 Phaethon) and high (2101 Adonis) value of ΔV_{min}.

Without using supplementary maneuvers, as, for example, enroute impulses or planetary flybys, the minimum ΔV required for a rendezvous mission is always greater than 3.5 km/s (more precisely, $\Delta V_{min} \simeq 3.56$ km/s for a mission towards asteroid 2000 EA14). The upper value of $\Delta V_{min} = 30$ km/s is reached in a rendezvous mission towards asteroid 2007 MB24. From Fig. 2, about 48% of the PHAs population requires a ΔV_{min} less than 10 km/s, while only 17% require a ΔV_{min} greater than 15 km/s. The latter value confirms the high cost of a rendezvous mission towards these celestial bodies. The analysis of the optimal initial angular position reveals that ν_0 increases almost linearly with the cumulative percent, thus implying the absence of a preferential value of ν_0 (this is due to the nearly circularity of Earth's orbit). A totally different result is obtained for the final position. In fact, about 58% of the asteroids population has an angular position $\nu_1 \in [140, 220]^\circ$. In other terms, the optimal transfer is obtained when the asteroid passes near its orbital aphelion, a result that is in agreement with the approximate analysis of Shoemaker and Helin [45] and of Izzo et al. [46].

[1] Available online at http://www.esa.int/gsp/ACT/inf/op/SemanticAsteroids/TheSemanticAsteroids.htm [Retrieved on November 23, 2009].

3.2. Minimum-time transfers using a canonical value of characteristic acceleration

Having obtained the database of PHAs as a function of the mission cost in terms of $\Delta V_{\min}$, minimum time rendezvous missions for an electric sail are now investigated. In all of the simulations, the 12 scalar differential equations (2) and (11) have been integrated in double precision using a variable order Adams–Bashforth–Moulton solver with absolute and relative errors of 10^{-12}. The value of characteristic acceleration, $a_c = 1\,\mathrm{mm/s^2}$, is, in analogy to what is usually done for solar sails, referred to as canonical characteristic acceleration, as it represents a reference value to establish the propulsion system performance. Although an accurate analysis of the electric sail subsystems is not yet available, preliminary studies suggest that the characteristic acceleration achievable in a near future is on the order of $2\,\mathrm{mm/s^2}$. A conservative estimate of a_c is about $0.5\,\mathrm{mm/s^2}$ [12]. However, very recent studies [47,48] suggest that a canonical value of characteristic acceleration may be compatible with the current technology. For example, assuming a payload mass (including the spacecraft bus) of 75 kg [22], the in-flight sailcraft total mass would be on the order of a few hundreds kilograms. In fact, using the mass breakdown model of Ref. [48], and assuming a total tether length 400 km (for example, fifty 8 km long tethers) the total mass is about 200 kg, with a payload mass fraction of 37.5%. The corresponding electric sail assembly mass (that is, the total in-flight mass except the payload) is 125 kg.

In addition, regarding the maximum value of allowable cone angle, a plasma dynamics simulation of an electric sail plunged into the solar wind has shown that $\alpha_{\max}$ is on the order of 35° [10,12]. For the sake of conservativeness, in all of the simulations a value of $\alpha_{\max} = 30^\circ$ has been assumed.

A problem that arises for the automated solution of a great number of optimal control problems is connected to the presence of local minimum points in the space of feasible results. In fact, it is important to recall that the theory of optimal control provides only necessary conditions for the existence of an optimum solution. This means that once the boundary conditions (22) associated with the optimal trajectory are met, the result found will be a local (but might not necessarily the global) minimum time corresponding to the given PHA orbit. From the simulations, the presence of local minima in the function $t_1 = t_1(\nu_0, \nu_1)$ is more likely to occur when the asteroid's orbits has a significant value of eccentricity (i.e., greater than 0.15). Clearly, the achievement of a local (rather than the global) minimum point in the optimization process depends on the initial guess of the optimization parameters, constituted by the adjoint variables $\lambda_p(t_0)$, $\lambda_f(t_0)$, $\lambda_g(t_0)$, $\lambda_h(t_0)$, $\lambda_k(t_0)$ and the true anomaly ν_0. To reduce the occurrence of such local minima, each Earth-asteroid mission has been optimized using a set of 20 different optimization parameters (that is, 20 different sets of the initial guess values), randomly chosen. The corresponding two-point boundary value problem (TPBVP) has been solved with boundary constraints set equal to 100 km for the position error and to 0.05 m/s for the velocity error. Finally, t_1 has been selected to be equal to the minimum value found in the 20 simulations of each mission. With such a procedure the optimization process of the whole database has been automated and a total of 20500 TPBVPs have been solved. The results in terms of minimum flight

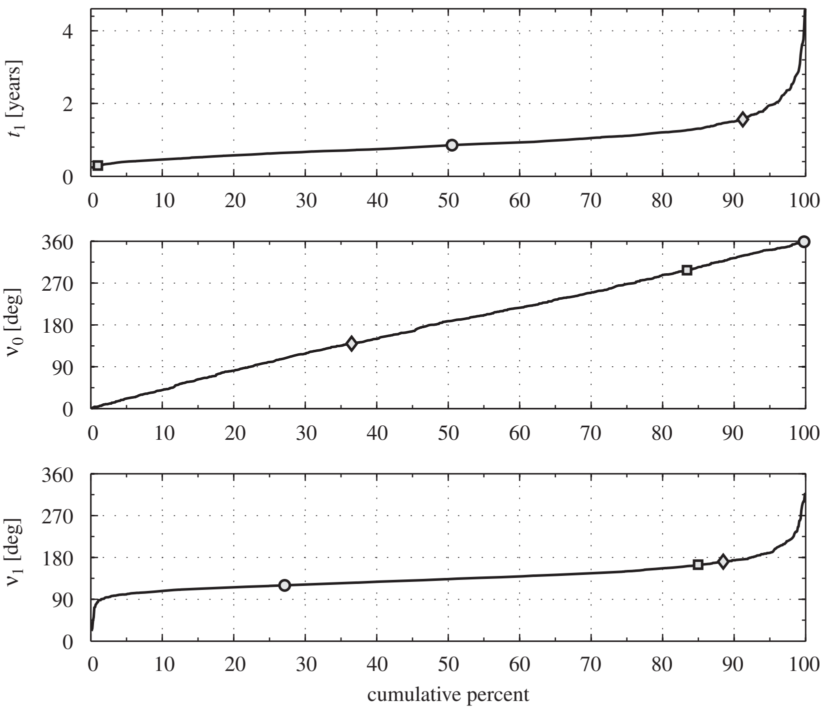

Fig. 3. Minimum-time Earth-PHA transfer using electric sail with $a_c = 1\,\mathrm{mm/s^2}$ (□ = 99942 Apophis, ◇ = 3200 Phaethon, ∘ = 2101 Adonis).

Table 1
Earth-PHA minimum transfer times for rapid missions ($t_1 \leq 180$ days).

Asteroid name	Two-impulse transfer			E-sail transfer		
	ΔV_{min} (km/s)	ν_0 (deg)	ν_1 (deg)	t_1 (days)	ν_0 (deg)	ν_1 (deg)
25143 Itokawa (1998 SF36)	4.252	132.0	210.5	86.87	139.8	88.0
(2002 AW)	4.121	165.8	195.1	87.60	227.6	127.4
(2006 KV89)	5.255	86.9	136.1	87.80	96.3	117.1
65679 (1989 UQ)	4.193	114.3	174.4	89.16	176.7	161.7
3361 Orpheus (1982 HR)	5.269	15.2	218.0	101.34	58.3	118.1
4660 Nereus (1982 DB)	4.968	10.7	219.1	101.77	6.1	88.0
(2002 RW25)	4.957	127.8	177.3	102.23	159.1	184.1
138404 (2000 HA24)	4.880	333.9	204.6	102.45	26.1	126.8
164202 (2004 EW)	5.744	335.4	147.1	102.79	355.2	148.0
99942 Apophis (2004 MN4)	4.335	165.6	199.6	106.85	297.5	164.4
(2004 PJ2)	5.836	131.8	237.3	107.55	142.7	98.3
(2000 SL10)	5.444	193.5	140.5	107.95	193.4	101.9
85585 Mjolnir (1998 FG2)	6.391	336.7	230.2	109.54	13.7	114.2
(2000 EA14)	3.566	305.5	144.2	111.48	323.8	116.3
(2003 YX1)	6.252	272.0	157.1	111.75	285.2	171.4
(2002 NV16)	3.672	259.3	189.1	112.99	253.4	93.6
(2000 QK130)	5.661	157.9	128.2	114.22	162.9	120.8
138175 (2000 EE104)	6.781	155.5	209.7	115.88	253.6	148.3
163364 (2002 OD20)	6.701	93.2	128.5	118.62	87.4	113.7
85990 (1999 JV6)	6.551	293.8	146.8	119.34	307.7	150.8
(2005 EE)	7.119	256.0	221.9	121.24	322.6	133.4
4581 Asclepius (1989 FC)	7.120	17.2	151.4	121.37	24.9	151.7
136618 (1994 CN2)	5.954	246.6	129.9	121.90	236.3	95.4
175706 (1996 FG3)	5.563	233.7	164.8	122.96	266.1	146.8
(2000 AC6)	5.273	193.5	171.1	123.36	262.0	179.3
(2001 FC58)	7.809	25.7	147.2	124.40	22.2	151.6
(1997 XR2)	6.178	263.5	112.5	125.20	258.4	132.8
(2006 SU49)	4.628	39.8	132.4	126.23	27.8	96.7
(2003 GY)	5.587	193.7	220.3	127.26	191.4	103.8
154019 (2002 CZ9)	7.042	142.1	129.3	127.41	138.3	120.1
152671 (1998 HL3)	5.466	250.0	169.8	129.69	282.4	140.2
152560 (1991 BN)	6.849	257.4	129.4	130.69	250.2	112.0
(2004 CO49)	6.328	318.6	219.9	131.65	334.7	116.7
(1998 HD14)	7.923	49.4	151.8	133.24	32.6	160.3
(2009 BL71)	6.541	145.2	204.8	133.43	260.1	165.0
154590 (2003 MA3)	6.168	294.1	163.2	134.25	317.2	146.6
(2002 LY1)	6.559	243.4	194.1	134.81	334.3	163.4
164211 (2004 JA27)	6.658	229.3	238.3	135.71	222.8	98.9
(1994 UG)	5.845	148.1	134.4	138.56	150.0	124.2
(2008 AO112)	5.634	333.2	208.0	138.90	333.4	114.1
89136 (2001 US16)	4.423	139.0	95.9	139.81	122.5	97.8
(2008 JG)	7.372	303.2	133.5	140.80	303.9	150.2
(2004 TP1)	8.325	44.5	125.9	141.11	34.5	130.9
(2005 WK4)	7.806	174.8	133.8	142.43	154.1	158.1
(2000 EW70)	7.056	150.5	203.3	142.54	252.2	167.0
(2001 XP31)	8.292	255.2	141.9	143.24	250.7	143.8
(2001 VB76)	6.149	48.6	112.7	144.66	34.1	106.9
(2008 WN2)	5.603	54.8	261.8	145.09	32.1	104.2
101955 (1999 RQ36)	5.095	329.4	113.2	145.13	323.7	124.0
(1994 CJ1)	5.441	135.0	105.1	145.27	117.2	99.6
5604 (1992 FE)	8.158	236.2	192.5	145.92	346.9	169.7
138971 (2001 CB21)	8.607	217.9	148.1	146.08	201.2	154.2
(2007 CN26)	6.337	196.4	234.2	147.60	188.2	114.2
(2006 XD2)	7.242	53.8	213.8	147.69	97.6	137.7
(2003 CC)	5.536	143.1	264.9	147.82	119.5	100.6
(2004 OB)	6.587	292.7	124.9	148.42	277.2	102.5
(2006 CU)	7.436	310.7	134.8	148.93	300.8	120.4
162000 (1990 OS)	6.390	265.6	158.6	149.31	255.2	109.1
(2006 SF6)	6.315	22.5	211.9	149.45	124.6	171.0
(2006 QQ23)	5.620	116.0	186.2	149.75	105.5	202.6
194006 (2001 SG10)	7.604	169.0	225.4	149.78	189.8	122.1
(2005 YO180)	8.192	11.2	126.5	149.87	358.1	123.1
6239 Minos (1989 QF)	7.386	150.6	154.5	150.07	157.6	148.4
(2003 DX10)	6.184	159.0	162.6	151.00	164.6	127.3
8014 (1990 MF)	6.866	217.2	226.7	151.08	207.8	104.5
(1999 YR14)	5.908	264.4	147.1	151.12	246.4	98.8

Table 1 (*continued*)

Asteroid name	Two-impulse transfer			E-sail transfer		
	ΔV_{min} (km/s)	ν_0 (deg)	ν_1 (deg)	t_1 (days)	ν_0 (deg)	ν_1 (deg)
(2004 QD14)	7.713	144.6	168.4	151.60	135.4	170.6
163249 (2002 GT)	6.815	228.6	229.1	152.14	230.6	118.4
(2008 UE7)	6.949	32.2	131.7	153.04	18.9	111.8
141432 (2002 CQ11)	7.496	215.1	192.4	153.28	299.7	165.6
(2006 BE55)	6.959	132.2	202.5	153.59	178.5	144.9
162361 (2000 AF6)	6.960	231.8	170.4	155.26	267.1	178.4
(2002 LT38)	6.025	274.6	193.1	155.32	24.0	189.5
(1999 AQ10)	6.406	103.0	212.7	156.11	211.7	174.5
(2005 MO13)	8.897	257.0	185.9	156.25	23.3	180.3
(2006 UQ17)	5.367	347.1	130.8	156.62	323.2	100.3
187040 (2005 JS108)	6.640	252.8	115.7	156.72	242.8	116.5
(2001 HY7)	7.371	349.8	162.7	156.81	9.6	175.0
(2006 WH1)	7.343	53.1	138.3	157.74	38.2	117.5
65717 (1993 BX3)	4.786	16.0	274.8	157.85	336.0	103.7
(1989 VB)	6.670	266.6	241.7	157.94	241.4	99.3
(2002 JX8)	5.822	158.2	173.4	158.67	12.9	204.3
140158 (2001 SX169)	6.932	82.8	158.3	158.94	86.8	137.4
153814 (2001 WN5)	6.888	222.5	143.9	160.02	208.2	111.6
162416 (2000 EH26)	6.592	134.9	162.6	160.21	117.1	105.8
(2000 CH59)	8.110	170.3	190.3	160.84	277.4	180.7
(2005 BY2)	6.919	98.0	231.0	161.16	110.4	131.4
(2003 YS17)	7.065	85.7	207.7	162.27	180.7	175.4
(2001 QC34)	4.483	20.7	135.0	162.61	22.3	132.6
(2005 ED318)	6.537	148.7	244.2	162.74	122.7	101.5
(2008 EV5)	4.490	162.3	134.1	163.12	259.1	173.9
(2008 KV2)	6.989	283.3	188.8	163.71	10.9	184.6
(2008 TD2)	5.934	234.2	247.5	164.04	205.1	103.9
(2000 UQ30)	6.920	354.4	129.5	164.10	336.2	108.4
155338 (2006 MZ1)	7.044	253.0	204.5	164.63	260.6	123.7
(2006 VG13)	7.262	189.9	184.4	164.73	175.4	198.7
(2002 JE9)	9.589	44.0	146.4	165.50	29.4	159.6
163348 (2002 NN4)	8.204	72.6	165.6	166.13	79.9	182.3
65803 Didymos (1996 GT)	6.144	294.2	248.4	166.89	261.8	103.0
(1998 HE3)	8.023	214.8	190.5	167.01	313.6	179.9
(2008 CN1)	6.747	228.6	173.0	167.10	297.5	200.1
(2000 KA)	8.989	74.4	139.8	167.36	61.9	140.6
162173 (1999 JU3)	4.315	349.3	133.5	167.38	341.4	120.1
136617 (1994 CC)	6.676	190.2	140.6	168.11	175.5	111.2
(2008 YS27)	5.250	356.7	141.9	168.69	331.1	105.1
85640 (1998 OX4)	7.878	300.9	221.6	168.87	310.8	124.7
(2006 GB)	6.732	33.4	126.2	169.20	357.0	174.0
(2003 WR21)	7.526	72.6	244.4	169.24	107.2	146.5
(1997 WQ23)	7.451	240.9	217.5	170.08	238.4	116.7
(1988 TA)	7.599	184.5	212.1	170.11	198.8	127.1
(2008 JV19)	6.084	306.8	218.7	170.38	23.9	169.3
(2008 HB38)	6.914	210.7	153.7	170.48	192.8	110.2
185851 (2000 DP107)	8.585	172.4	239.5	170.67	186.6	128.9
(1989 UP)	6.782	324.4	136.8	170.74	302.6	105.6
(2002 OA22)	5.778	343.4	213.1	171.03	77.9	182.6
(2003 BR47)	8.045	311.4	222.5	172.93	319.8	124.8
192559 (1998 VO)	7.749	233.3	114.8	173.05	219.5	153.6
(2005 CJ)	7.259	344.0	153.6	173.25	329.6	121.6
162998 (2001 SK162)	6.554	8.5	153.8	173.96	340.3	103.5
(2002 DU3)	6.963	159.6	118.1	174.46	155.5	144.6
(2001 PT9)	9.098	151.6	129.7	174.51	136.3	132.2
6037 (1988 EG)	8.073	343.9	155.1	174.62	344.4	148.4
152754 (1999 GS6)	7.420	329.1	194.8	174.76	16.6	154.2
(2005 LW3)	8.627	223.5	222.2	174.82	248.4	133.2
163697 (2003 EF54)	6.751	160.2	191.2	175.23	156.4	123.8
(2006 HC2)	7.923	172.0	135.1	177.01	155.2	120.4
(2005 GD60)	9.287	176.0	242.6	177.07	199.9	134.5
153958 (2002 AM31)	6.822	237.3	149.5	177.26	221.6	114.1
35396 (1997 XF11)	8.336	194.2	213.7	177.36	220.7	135.5
(2000 YF29)	6.397	50.4	138.7	177.75	34.0	118.2
(2006 TU7)	8.423	108.6	171.8	178.16	118.0	186.8
(1999 UR)	7.043	324.7	147.1	179.30	304.5	112.0
(2001 TX1)	7.045	48.4	186.3	179.59	94.1	166.9

Table 1 (*continued*)

Asteroid name	Two-impulse transfer			E-sail transfer		
	ΔV_{min} (km/s)	ν_0 (deg)	ν_1 (deg)	t_1 (days)	ν_0 (deg)	ν_1 (deg)
(1991 JW)	5.409	261.4	241.2	179.73	250.0	147.6
(2001 SG286)	7.527	199.8	123.8	180.30	189.3	128.8
(2007 SQ6)	5.826	19.6	257.4	180.30	21.8	156.5
(2002 AT4)	6.461	62.8	122.9	180.48	35.2	105.0

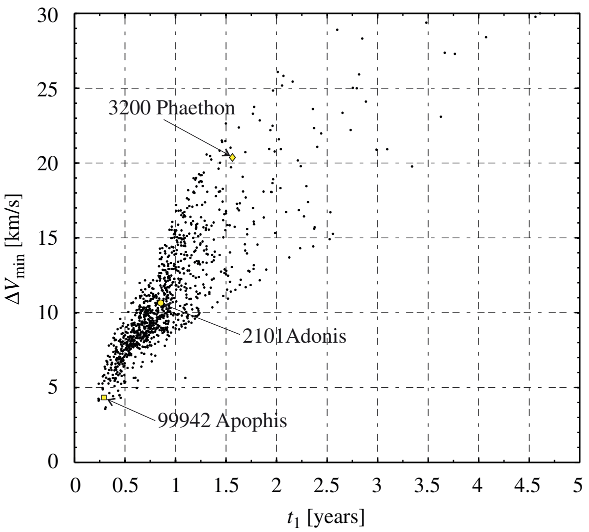

Fig. 4. E-sail minimum flight time (t_1) vs. two-impulse ΔV_{min} ($\square$ = 99942 Apophis, $\diamond$ = 3200 Phaethon, $\circ$ = 2101 Adonis).

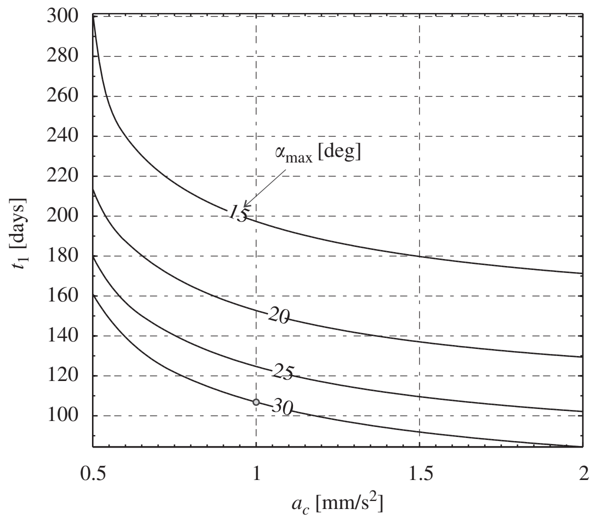

Fig. 5. Mission towards asteroid 99942 Apophis: minimum transfer times t_1 as a function of a_c and α_{max}. The gray point represents the case discussed in the text.

times and optimal initial and final angular positions are given in detail in the table attached to this paper in electronic form. The same results are also summarized in graphical form, in terms of cumulative percent, in Fig. 3.

For the whole population of PHAs the flight times are always less than 4.6 years. This is a reasonable time, even the more so if one recalls that the missions are completed without any intermediate flyby maneuver. A noteworthy result is that about 67% of PHAs may be reached with a total mission time less than one year, while 4% only requires times greater than two years. For example, a rendezvous mission towards 25143 Itokawa goes on for 87 days, while 570 days are sufficient to reach 3200 Phaethon. As for the optimal initial and final angular positions, the electric sail option provides results very similar to the previously discussed two-impulse transfer. The electric sail has the potential to guarantee the fulfilment of rapid rendezvous missions, with times less than six months, to 137 asteroids, corresponding to about 14% of the whole population. The mission performance for this subset of PHAs is shown in Table 1 along with the corresponding ΔV values for a two-impulse transfer. The table rows have been ordered as a function of the increasing mission time for the electric sail option.

The potential of the electric sail for PHAs missions is also clearly shown in Fig. 4 in which, for each mission, the minimum flight time is represented as a function of the ΔV_{min} found with a two impulse strategy. Fig. 4 shows that the electric sail may reach, within reasonable times (that is, less than four years), asteroids that otherwise would require $\Delta V_{min} \simeq 30\,\mathrm{km/s}$, a value comparable to the Earth's mean orbital velocity.

4. Case study: rendezvous with asteroid 99942 Apophis

A mission analysis towards asteroid 99942 Apophis represents a reference case study to evaluate the performance of a given propulsion system. Our aim now is to conduct a parametric investigation to analyze the electric sail capabilities (in terms of mission times) for different values of both the characteristic acceleration and the maximum cone angle. Assuming a variation range $a_c \in [0.5, 2]\,\mathrm{mm/s^2}$ and $\alpha_{max} \in [15, 30]^\circ$, the isocontour lines for the minimum flight times are illustrated in Fig. 5. As is clear from the figure, there is a strong dependence of t_1 from a_c, especially for $a_c < 0.7\,\mathrm{mm/s^2}$ (note, in fact, that the curves $t_1 = t_1(a_c)$ have a vertical asymptote when $a_c \to 0$). The flight time has a certain dependence on the

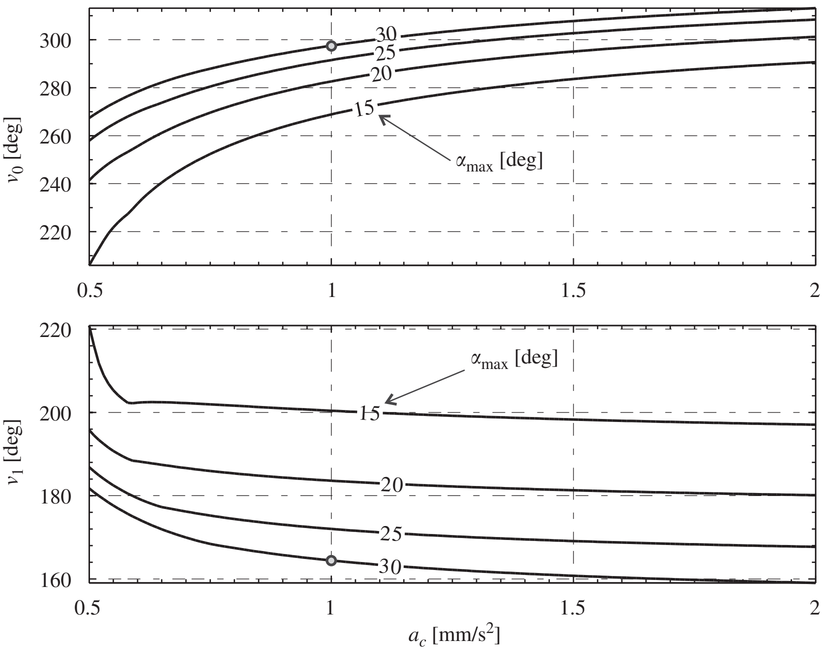

Fig. 6. Mission towards asteroid 99942 Apophis: optimal initial (v_0) and final (v_1) sailcraft position as a function of a_c and α_{max}. The gray point represents the case discussed in the text.

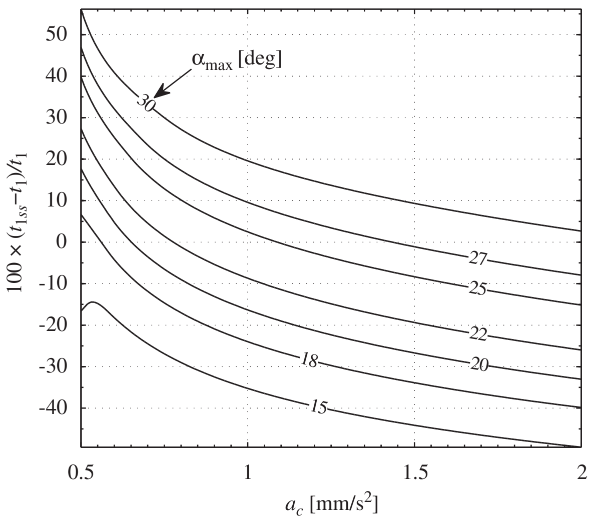

Fig. 7. Minimum-time mission towards asteroid 99942 Apophis: comparison between electric sail (t_1) and flat solar sail ($t_{1_{ss}}$).

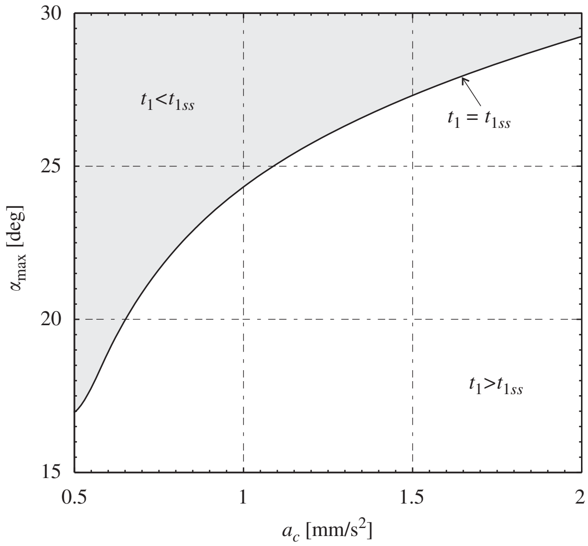

Fig. 8. Electric sail vs. solar sail performance for minimum-time mission towards asteroid 99942 Apophis.

maximum allowed value of the cone angle, however such a dependence is weak when $\alpha_{max} > 20^\circ$. The optimal initial and final angular positions are shown in Fig. 6.

Assuming $a_c = 1\,\mathrm{mm/s^2}$ and $\alpha_{max} = 30^\circ$, from Figs. 5 and 6 one obtains that $t_1 \simeq 107$ days, $v_0 = 297.5^\circ$ and $v_1 = 164.4^\circ$ (see also Table 1). For comparative purposes, a flat solar sail with the same characteristic acceleration will require a flight time of 128 days [24], an increase of 18% with respect to an electric sail. Using the same value of characteristic acceleration for a solar and an electric sail, one may obtain a reasonable comparison between the performance of these two different propulsion systems in terms of mission times. The mathematical model and the performance characteristics for a flat solar sail with an optical force model are described in detail in Refs. [24,36,49]. With such a model, the optimal mission times $t_{1_{ss}}$ towards asteroid 99942 Apophis have been calculated with v_0 and v_1 left free. The differences in flight times between the two propulsion systems (electric and solar sail) as a function of a_c and α_{max} are illustrated in Fig. 7. Electric sails have lower times of flight when

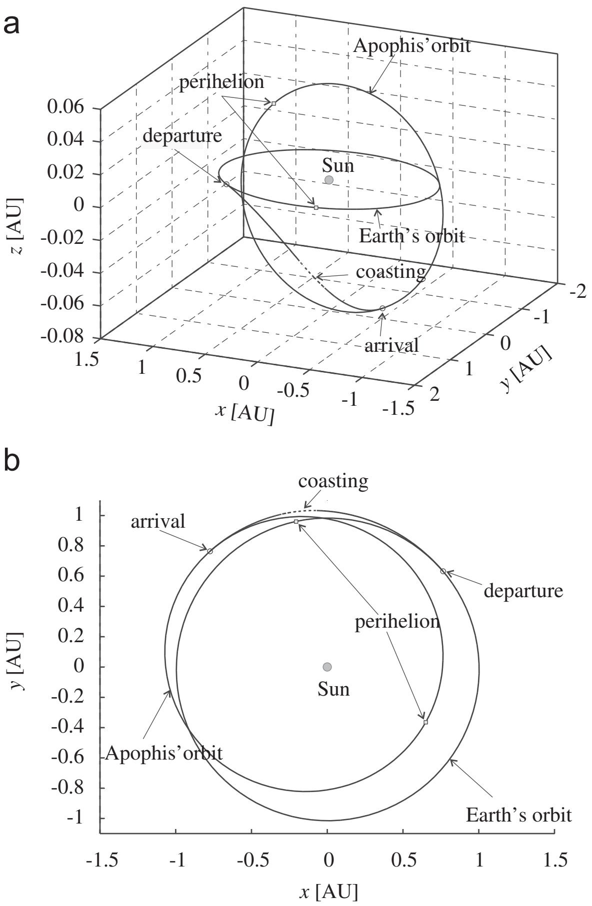

Fig. 9. Optimal Earth-Apophis trajectory with $a_c = 1\,\mathrm{mm/s^2}$ and $\alpha_{max} = 30^\circ$. (a) Three-dimensional view. (b) Ecliptic projection.

compared to solar sails for lower characteristic accelerations (a_c) and higher α_{max}.

For a given value of characteristic acceleration, the difference $t_1 - t_{1_{ss}}$ decreases remarkably as α_{max} is decreased. In other terms, the reduced maneuver capability of an electric sail associated to a reduction in α_{max}, significantly penalizes the flight time. Clearly, there exists a suitable pair (a_c, α_{max}) such that the performance of a solar sail coincides with that of an electric sail. In mathematical terms, the condition $t_1 = t_{1_{ss}}$ is illustrated in Fig. 8. The curve $a_c = a_c(\alpha_{max})$ plotted in Fig. 8 characterizes all the pairs (a_c, α_{max}) such that the electric sail is superior, in terms of shorter mission times, to a flat solar sail (gray region) with an optical force model. Assuming $a_c = 1\,\mathrm{mm/s^2}$ and $\alpha_{max} = 30^\circ$, the transfer trajectory for an electric sail is illustrated in Fig. 9.

Fig. 9(b) shows the existence of a coasting phase ($\tau = 0$), of about $t_c \simeq 15$ days ($t_c/t_1 \simeq 14\%$), in the optimal trajectory. This phase, which is absent in a solar sail based transfer [24], is closely related to the constraint on the upper value of the cone angle. In fact, during the whole mission length the cone angle always maintains its maximum admissible value (see Fig. 10), and the reduced maneuver capability imposed by α_{max} is compensated, in part, by the introduction of an optimal coasting phase.

Moreover, a decrease in the value of α_{max} causes an increase in the coasting length t_c. This is confirmed by the results of Fig. 11, which also emphasizes a dependence of t_c on the value of a_c. In particular, an increase in a_c tends to increase the ratio t_c/t_1. In fact, in the limit as $a_c \to \infty$, the sailcraft trajectory becomes a conic ($t_c/t_1 = 1$) and one obtains a two-impulse maneuver.

4.1. Optimal transfers with constraints on sailcraft initial position

So far the simulation results have been obtained with both v_0 and v_1 left free. Assuming to fix the initial sailcraft position on the initial orbit, that is, to assign a launch date, it is possible to calculate the optimal mission performance for this case with minor modifications to the previous mathematical model. More precisely, the boundary condition $\lambda_L(t_0) = 0$ in Eq. (22) is now substituted by the new condition $L(t_0) = \Omega_\oplus + \omega_\oplus + v_0$. When the optimal control problem is solved for different values of the characteristic acceleration and $\alpha_{max} = 30^\circ$, the simulation results are illustrated in Fig. 12.

For a given value of a_c, the curve $t_1 = t_1(v_0)$ shows the presence of both a local and a global minimum. The latter value is coincident with the results of Fig. 5 and of Table 1. Note the rapid variation of the function $t_1 = t_1(v_0)$ in the nearness of the global minimum, a behavior similar to that found for a solar sail and discussed in Ref. [24].

5. Conclusions

A thoroughly investigation of the potentialities of an electric sail for mission towards PHAs has been presented. A total of 1025 missions have been studied in an optimal framework, by minimizing the total mission time with an indirect approach. Assuming a canonical value of characteristic acceleration, about 67% of the asteroids may be reached within one year of mission time, and 137 within six months. Although these results may be optimistic, because they have been obtained with open initial and final sailcraft positions (that is, without taking into account the actual ephemeris constraints), nevertheless they clearly show the potentialities of an electric sail. Moreover, a detailed study towards asteroid 99942 Apophis has been conducted by varying both the value of the characteristic acceleration and that of the maximum value of the cone angle and a comparison with the corresponding performance achievable with a solar sail has been discussed. From the obtained results, the electric sail appears as a very promising advanced propulsion system and an intriguing alternative to a solar sail for small-body exploration.

Acknowledgment

The authors are indebted to Pekka Janhunen for his useful comments about this paper.

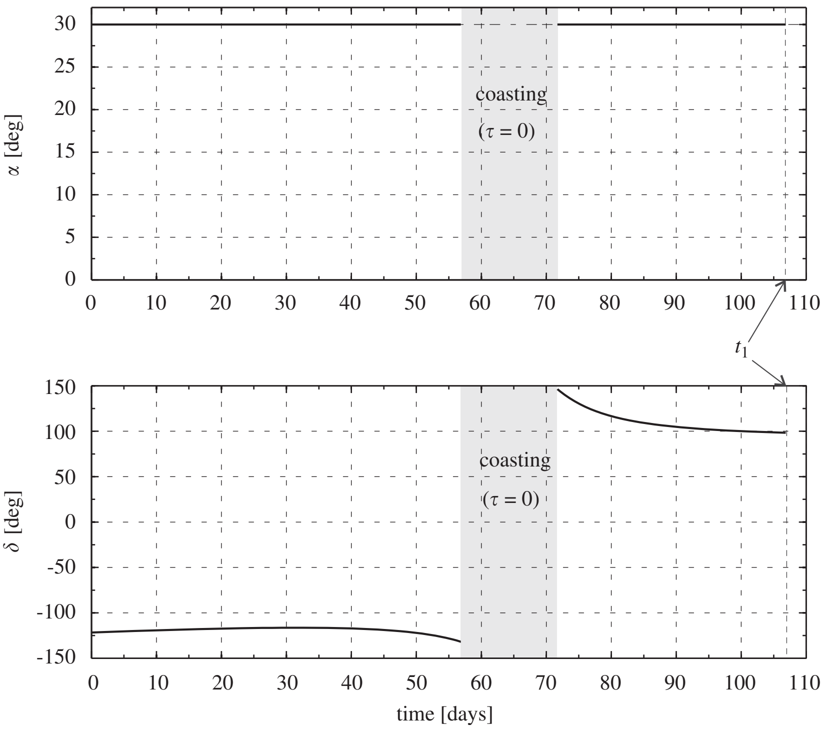

Fig. 10. Mission towards asteroid 99942 Apophis: optimal control angles ($a_c = 1\,\mathrm{mm/s^2}$ and $\alpha_{max} = 30^\circ$).

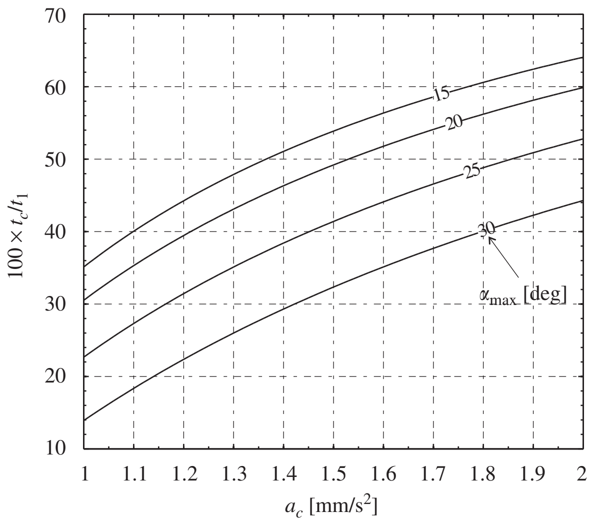

Fig. 11. Coasting time t_c as a function of a_c and α_{max} for mission towards asteroid 99942 Apophis.

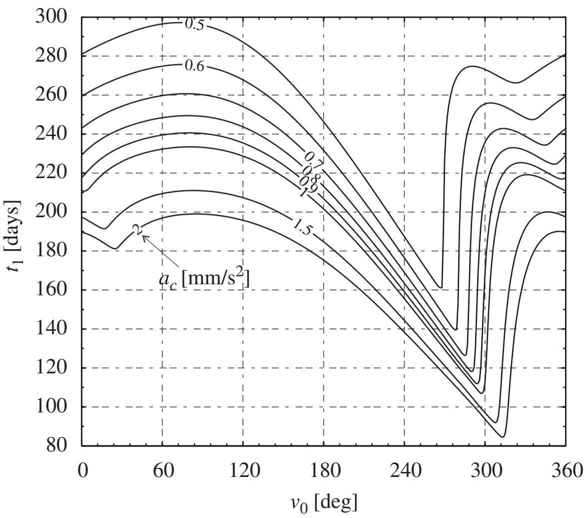

Fig. 12. Mission towards asteroid 99942 Apophis: minimum transfer time t_1 as a function of a_c and ν_0 ($\alpha_{max} = 30^\circ$).

Appendix A. Analytical expressions of A and $\boldsymbol{b}$

According to Betts [32], the non-zero entries of A and $\boldsymbol{b}$, defined in Eq. (2), are A_{12}, A_{21}, A_{22}, A_{23}, A_{31}, A_{32}, A_{33}, A_{43}, A_{53}, A_{63}, and b_6. An explicit expression for A_{ij} and b_6 as a function of the MEOE is [32]

$$A_{12} = \frac{2p}{1+f\cos L+g\sin L}\sqrt{\frac{p}{\mu_\odot}} \tag{23}$$

$$A_{21} = \sin L\sqrt{\frac{p}{\mu_\odot}} \tag{24}$$

$$A_{22} = \frac{(2+f\cos L+g\sin L)\cos L+f}{1+f\cos L+g\sin L}\sqrt{\frac{p}{\mu_\odot}} \tag{25}$$

$$A_{23} = -\frac{g(h\sin L-k\cos L)}{1+f\cos L+g\sin L}\sqrt{\frac{p}{\mu_\odot}} \tag{26}$$

$$A_{31} = -\cos L\sqrt{\frac{p}{\mu_\odot}} \tag{27}$$

$$A_{32} = \frac{(2+f\cos L+g\sin L)\sin L+g}{1+f\cos L+g\sin L}\sqrt{\frac{p}{\mu_\odot}} \tag{28}$$

$$A_{33} = \frac{f(h\sin L-k\cos L)}{1+f\cos L+g\sin L}\sqrt{\frac{p}{\mu_\odot}} \tag{29}$$

$$A_{43} = \frac{(1+h^2+k^2)\cos L}{2(1+f\cos L+g\sin L)}\sqrt{\frac{p}{\mu_\odot}} \tag{30}$$

$$A_{53} = \frac{(1+h^2+k^2)\sin L}{2(1+f\cos L+g\sin L)}\sqrt{\frac{p}{\mu_\odot}} \tag{31}$$

$$A_{63} = \frac{h\sin L-k\cos L}{1+f\cos L+g\sin L}\sqrt{\frac{p}{\mu_\odot}} \tag{32}$$

and

$$b_6 = \sqrt{\mu_\odot p}\left(\frac{1+f\cos L+g\sin L}{p}\right)^2 \tag{33}$$

Appendix B. Supplementary data

Supplementary data associated with this article can be found in the online version at doi:10.1016/j.actaastro.2009.11.021.

References

[1] R.L. Schweickart, Decision program on asteroid threat mitigation, Acta Astronautica 65 (9–10) (2009) 1402–1408.
[2] J.L. Remo, Characterizing the near-earth object hazard and its mitigation, Acta Astronautica 50 (12) (2002) 737–746.
[3] A. Hanslmeier, The Sun and Space Weather, Astrophysics and Space Science Library, Kluwer Academic Publishers, New York, 2004 (Chapter 11, pp. 202–203, ISBN 978-1-4020-0684-5 (Print) 978-0-306-48211-3 (Online)).
[4] J.L. Remo, A quantitative NEO hazard mitigation scale, Acta Astronautica 54 (10) (2004) 755–762.
[5] D.J. Korsmeyer, R.R. Landis, P.A. Abell, Into the beyond: a crewed mission to a near-earth object, Acta Astronautica 63 (1–4) (2008) 213–220.
[6] A. Phipps, M. Meerman, J. Wilhelm, D. Gibbon, J. Northam, A. da Silva Curiel, J. Ward, M. Sweeting, An 'entry level' mission to a near earth object, Acta Astronautica 59 (8–11) (2006) 845–857.
[7] J.L. Remo, Energy requirements and payload masses for near-earth objects hazard mitigation, Acta Astronautica 47 (1) (2000) 35–50.
[8] D.D. Mazanek, C.M. Roithmayr, J. Antol, L. Kay-Bunnell, M.R. Werner, S.-Y. Park, R.R. Kumar, Comet/asteroid protection system (CAPS): a space-based system concept for revolutionizing earth protection and utilization of near-earth objects, Acta Astronautica 53 (4–10) (2003) 405–422.
[9] P. Janhunen, Electric sail for spacecraft propulsion, Journal of Propulsion and Power 20 (4) (2004) 763–764.
[10] P. Janhunen, A. Sandroos, Simulation study of solar wind push on a charged wire: basis of solar wind electric sail propulsion, Annales Geophysicae 25 (3) (2007) 755–767.
[11] P. Janhunen, The electrical sail—a new propulsion method which may enable fast missions to the outer solar system, Journal of the British Interplanetary Society 61 (2008) 322–325.
[12] G. Mengali, A.A. Quarta, P. Janhunen, Electric sail performance analysis, Journal of Spacecraft and Rockets 45 (1) (2008) 122–129.
[13] P. Janhunen, On the feasibility of a negative polarity electric sail, Annales Geophysicae 27 (4) (2009) 1439–1447.
[14] G. Mengali, A.A. Quarta, P. Janhunen, Considerations of electric sailcraft trajectory design, Journal of the British Interplanetary Society 61 (2008) 326–329.
[15] G. Mengali, A.A. Quarta, Non-Keplerian orbits for electric sails, Celestial Mechanics and Dynamical Astronomy 105 (1–3) (2009) 179–195.
[16] R.W. Farquhar, D.W. Dunham, J.V. McAdams, NEAR mission overview and trajectory design, Journal of the Astronautical Sciences 43 (4) (1995) 353–371.
[17] D. Qiao, H. Cui, P. Cui, Evaluating accessibility of near-earth asteroids via earth gravity assists, Journal of Guidance, Control, and Dynamics 29 (2) (2006) 502–505.
[18] R.W. Farquhar, D.W. Dunham, J.V. McAdams, Comment on "evaluating accessibility of near-earth asteroids via earth gravity assists", Journal of Guidance, Control, and Dynamics 29 (6) (2006) 1485.
[19] M. Morimoto, H. Yamakawa, M. Yoshikawa, M. Abe, H. Yano, Trajectory design of multiple asteroid sample return missions, Advances in Space Research 34 (2004) 2281–2285.
[20] J.V. McAdams, Postlaunch contingency trajectories for the near-earth asteroid rendezvous mission, Journal of Guidance, Control, and Dynamics 20 (4) (1997) 819–823.
[21] B. Dachwald, W. Seboldt, Solar sailcraft of the first generation mission applications to near-Earth asteroids, in: 54th International Astronautical Congress, IAC-03-Q.5.06, Bremen, Germany, 2003.
[22] B. Dachwald, W. Seboldt, Multiple near-earth asteroid rendezvous and sample return using first generation solar sailcraft, Acta Astronautica 57 (11) (2005) 864–875.
[23] B. Dachwald, B. Wie, Solar sail kinetic energy impactor trajectory optimization for an asteroid-deflection mission, Journal of Spacecraft and Rockets 44 (4) (2007) 755–764.
[24] G. Mengali, A.A. Quarta, Rapid solar sail rendezvous missions to asteroid 99942 Apophis, Journal of Spacecraft and Rockets 46 (1) (2009) 134–140.
[25] E. Morrow, D.J. Scheeres, D. Lubin, Solar sail orbit operations at asteroids, Journal of Spacecraft and Rockets 38 (2) (2001) 279–286.
[26] D.F. Bender, R.D. Bourke, Multiasteroid comet missions using solar electric propulsion, Journal of Spacecraft and Rockets 10 (8) (1973) 481–482.
[27] R.M. Winglee, J. Slough, T. Ziemba, A. Goodson, Mini-magnetospheric plasma propulsion: tapping the energy of the solar wind for spacecraft propulsion, Journal of Geophysical Research 105 (A9) (2000) 21067–21078.
[28] G. Mengali, A.A. Quarta, Optimal missions with minimagnetospheric plasma propulsion, Journal of Guidance, Control, and Dynamics 29 (1) (2006) 209–212.
[29] G. Mengali, A.A. Quarta, Minimagnetospheric plasma propulsion for outer planet missions, Journal of Guidance, Control, and Dynamics 29 (5) (2006) 1239–1242.
[30] M.J.H. Walker, J. Owens, B. Ireland, A set of modified equinoctial orbit elements, Celestial Mechanics 36 (1985) 409–419.
[31] M.J. Walker, Erratum—a set of modified equinoctial orbit elements, Celestial Mechanics 38 (1986) 391–392.
[32] J.T. Betts, Very low-thrust trajectory optimization using a direct SQP method, Journal of Computational and Applied Mathematics 120 (1) (2000) 27–40.
[33] V.L. Coverstone, J.E. Prussing, Technique for escape from geosynchronous transfer orbit using a solar sail, Journal of Guidance, Control, and Dynamics 26 (4) (2003) 628–634.
[34] C.R. McInnes, Solar Sailing: Technology, Dynamics and Mission Applications, in: Springer-Praxis Series in Space Science and Technology, Springer, Berlin, 1999, pp. 46–54.
[35] J.L. Wright, Space Sailing, Gordon and Breach Science Publisher, Berlin, 1992, pp. 223–226.
[36] G. Mengali, A.A. Quarta, Optimal control laws for axially symmetric solar sails, Journal of Spacecraft and Rockets 42 (6) (2005) 1130–1133.
[37] G. Mengali, A.A. Quarta, Solar sail near-optimal circular transfers with plane change, Journal of Guidance, Control, and Dynamics 32 (2) (2009) 456–463.
[38] J.A. Kechichian, Optimal low-thrust rendezvous using equinoctial orbit elements, Acta Astronautica 38 (1) (1996) 1–14.
[39] G. Mengali, A.A. Quarta, Fuel-optimal, power-limited rendezvous with variable thruster efficiency, Journal of Guidance, Control, and Dynamics 28 (6) (2005) 1194–1199.
[40] G. Mengali, A.A. Quarta, Optimal three-dimensional interplanetary rendezvous using nonideal solar sail, Journal of Guidance, Control, and Dynamics 28 (1) (2005) 173–177.
[41] Jet propulsion laboratory: near earth object program [Retrieved on March 20, 2009]. ⟨http://neo.jpl.nasa.gov/⟩.

[42] C.O. Lau, N.D. Hulkower, Accessibility of near-earth asteroids, Journal of Guidance, Control, and Dynamics 10 (3) (1987) 225–232.
[43] N.D. Hulkower, C.O. Lau, D.F. Bender, Optimum two-impulse transfers for preliminary interplanetary trajectory design, Journal of Guidance, Control, and Dynamics 7 (4) (1984) 458–461.
[44] J.C. Lagarias, J.A. Reeds, M.H. Wright, P.E. Wright, Convergence properties of the Nelder–Mead simplex method in low dimensions, SIAM Journal on Optimization 9 (1) (1998) 112–147.
[45] E.M. Shoemaker, E.F. Helin, Earth-approaching asteroids as targets for exploration, in: D. Morrison, W.C. Wells (Eds.), Asteroids: An Exploration Assessment, NASA Conference Publication 2053, The University of Chicago, 1978, pp. 245–256, NASA CP-2053. 〈http://ntrs.nasa.gov/archive/nasa/casi.ntrs.nasa.gov/19780021064_1978021064.pdf〉.
[46] D. Izzo, T. Vinkó, C. Bombardelli, S. Brendelberger, S. Centuori, Automated asteroid selection for a grand tour mission, in: 58th International Astronautical Congress, Hyderabad, India, 2007, paper IAC-07-C1.7.07.
[47] P. Janhunen, Increased electric sail thrust through removal of trapped shielding electrons by orbit chaotisation due to spacecraft body, Annales Geophysicae 27 (8) (2009) 3089–3100.
[48] A.A. Quarta, G. Mengali, Electric sail mission analysis for outer solar system exploration, Journal of Guidance, Control, and Dynamics, in press, doi: 10.2514/1.47006.
[49] G. Mengali, A.A. Quarta, C. Circi, B. Dachwald, Refined solar sail force model with mission application, Journal of Guidance, Control, and Dynamics 30 (2) (2007) 512–520.